Investigating the influence of fines in fluidized bed reactors using 3D ECT images

C. Rautenbach, M. C. Melaaen & B. M. Halvorsen
Institute for Process, Energy and Environmental Technology, Telemark University College, Norway

Abstract

Electrical Capacitance Tomography (ECT) has become a useful measurement tool in process technology applications, especially in fluidized bed research. The ECT system is neither intrusive nor invasive which make the system practically viable for monitoring the internal flow behaviour in a fluidized bed. The sensor is placed on the outside of the non-conductive experimental reactor thus making implementation very convenient. ECT also presents user friendly equipment that is safe and easy to use compared to some of the other tomographic modalities currently available.

There has been postulated that the insertion of fines into a powder will give more uniform flow behaviour in a fluidized bed. Smaller and more evenly distributed bubbles are observed. These conditions lead to better mixing of gas and solids in a fluidized bed and thus improving the reactions in the reactor. These phenomena have been investigated in the present study using ECT and a reconstruction program developed in the present study. This reconstruction program created three dimensional images of the fluidized bed reactor under consideration. The reconstructions allow the user to get a three dimensional visual image of the flow behaviour inside the experimental reactor without disturbing the flow. Bubble- and bed characteristics of several powders with different percentages of fines were investigated. The volume, location and shape of individual bubbles were studied and thus the average bubble size, volume and frequency of a particular experimental set up was calculated. These quantities are of great importance for numerous industrial applications. Applications of these results are in almost all fields involving fluidization. The research is part of ongoing global research in optimizing and understanding fluidized beds better.

WIT Transactions on Engineering Sciences, Vol 70, © 2011 WIT Press
www.witpress.com, ISSN 1743-3533 (on-line)
doi:10.2495/MPF110121

The results are given, and its concluded that the insertion of fines into a powder would have the effect of smaller bubbles and cause Geldart type **D** powders to be less prone to slugging behaviour.
Keywords: fluidization, ECT, fines, bubble characteristics.

1 Introduction

Process tomography has been used to visualise internal flow behaviour of numerous industrial processes [1]. In the past intrusive techniques were used in an attempt to visualise flow processes that would otherwise not lend it self to be studied visually. The problem with such intrusive measuring techniques is that they alter the normal flow behaviour of the process. Doubts thus arises whether the recorded data is an accurate reflection of how that process would otherwise behave, react or change. In fluidized beds the flow behaviour is of great importance. The better a rector can be understood the better predictions can be made of its behaviour. Optimizing these reactors' mixing capabilities increases production and thus cost effectiveness. Better modeling and non-intrusive measurements of bubbling behaviour, mixing and circulation properties can have a drastic impact on optimizing fluidized bed reactors. With this in mind the influence of fine in a fluidized bed reactor was investigated in the present study using the ECT system and a reconstruction program developed for the present study.

1.1 The ECT system

A two plane ECT system was used in the present study. It consists of two arrays of electrodes and each array contains twelve electrodes. In Figure 1(a) a schematic drawing of the ECT sensor is given. The location and size of the electrodes were designed by Process Tomography Ltd. [2]. The sensor is covered by a grounded screen to protect the electrodes from external noise because the sensor operates with a soft field and is very susceptible to external interference. The non-invasive neither intrusive nature of the sensor can be observed in Figure 1(b). The electrodes are placed on the circumference of the experimental tower and thus does not influence the internal flow behaviour. The ECT system produces a cross-sectional image showing the distribution of electrical permittivities of the content of the experimental tower from measurements taken at the boundary of the vessel [3]. The capacitance reading is taken between each set of electrodes and thus $n/2(n-1)$ different capacitance values are recorded in one measurement, where n is the number of electrodes. These measurements are interpreted and illustrated as a colourful image using a reconstruction algorithm provided by Process Tomography Ltd. [2]. An example of an image depicting the solid fraction distribution in a fluidized bed is given in Figure 2(b). The resolution of the image is usually relatively low but can be sampled at high sample rates. Off-line image processing can also improve the quality of the image dramatically [4].

The measuring planes are situated at two different locations. One at height of 156.5 mm and the other at a height of 286.5 mm above the gas distributor. The

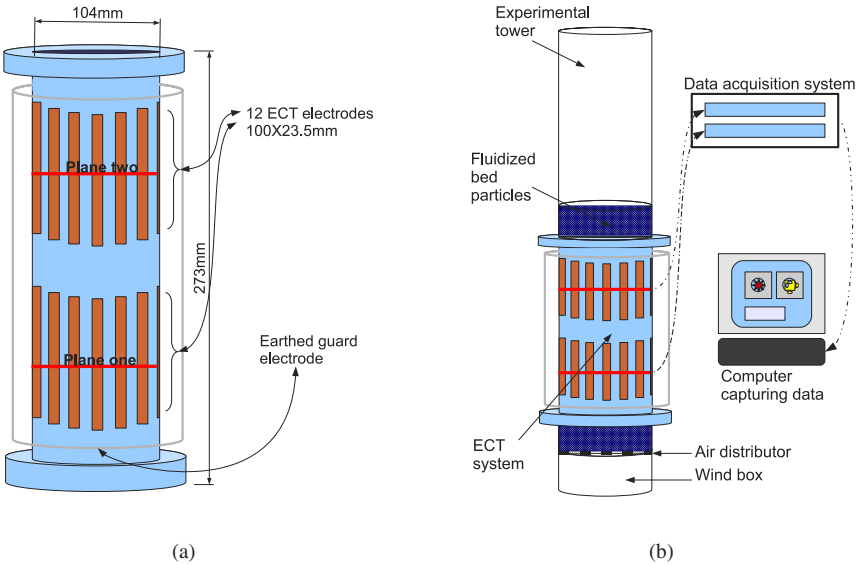

Figure 1: A not to scale drawing of the two plane ECT system utilised in the present study. (a) The two measuring planes of the system are indicated together with the electrodes and earthed guard screen. (b) The ECT system together with the experimental tower, acquisition system and the computer recording the data.

lower plane will be called plane one and the upper plane, plane two (refer to Figure 1(a)). Even though the ECT system calculates averages, the data that are obtained are viewed as a slice through the bed at the center of each sensor. Plane one and plane two is thus located at the center position of the electrodes (refer to Figure 1(a)).

The obtained image consists of pixels and each pixel represents an average solid fraction value. The average is taken over a rectangular volume equal to $9.77\times10^{-7}m^3$ [3]. A 32×32 pixel image is produced and the pixels that falls outside the circular tower will assume zero values (refer to Figure 2).

Theoretically, the more electrodes one uses the smaller the electrodes become and the more dominant the background noise can become. Thus a trade of has to be made so that the electrode is not too small but also not too large. When the electrodes are too large the resolution of the produce image will be very low. The system with twelve electrodes can capture up to a hundred 32×32 matrix maps of solid fractions per second and increasing to two hundred frames per second for an eight electrode sensor [3]. Practically between six and sixteen electrodes are normally used [2].

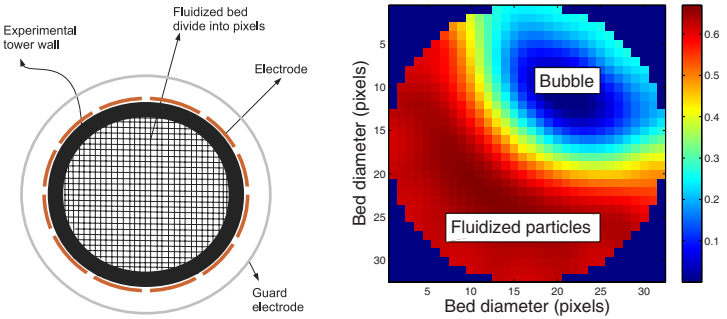

(a) (b)

Figure 2: (a) A cross-sectional view of the ECT sensor together with the 1024 pixels created by the reconstruction program and (b) a cross-sectional image of the experimental tower indicating the solid fraction values inside the tower at a particular plane. Red indicates particles at minimum fluidization conditions and blue indicates air.

1.2 Experimental set-up and procedure

This system also requires calibration. First the tower is left empty so that just air is present. The ECT software then calibrates this as the low permittivity material (the blue colour in Figure 2(b)). Then the tower is filled with the powder that is investigated and the ECT software calibrates this as the high permittivity material (the red colour in Figure 2(b)) [2]. This provides the reconstruction algorithm the necessary boundary conditions to accurately represent the permittivities in-between these two extreme values.

A series of four powder and powder mixes were used during the present study. The characteristics of the investigated powders are presented in Table 1. For convenience abbreviations will be used in the figures and they are as follows: the mixture containing fifty percent 100–200μm powder and fifty percent 400–600μm will be called '*mix 1*' and the mixed powder containing eighty three percent of the 750–1000μm powder and eight and a half percent 400–600μm and 100–200μm powder respectively will be called '*mix 2*'. The mean particle diameter was calculated using the *surface-volume mean* diameter and is defined as

$$\overline{d}_{sv} = \frac{1}{\sum_i x_i/d_i}, \tag{1}$$

with x_i the mass fraction of the particular particle size and d_i the particular particle size. The minimum fluidization velocity (u_{mf}) was determined using either pressure drop measurements or the standard deviation of the average solid

Table 1: Relevant parameters of the powders used in the present study.

Powders used	Mean particle size ($\overline{d}_{sv}$) [μm]	Solid fraction (ϵ_s) [-]	u_{mf} [m/s]
100–200μm	153 [5]	0.68	0.022
400–600μm	482.9	0.68	0.21 [6]
750–1000μm	899.15	0.67	0.42 [6]
mix 1 : 50% 100–200μm, 50% 400–600μm	265.58	0.66	0.037
mix 2 : 8.5% 100–200μm, 8.5% 400–600μm, 83% 750–1000μm	-	0.7	0.27

fraction measurements or both [4]. Both methods are acceptable and the values obtained agrees significantly.

Gas was fed into the $10.4cm$ experimental tower through a porous plate distributor. Air was used as fluidizing fluid and all of the powders mentioned in Table 1 were made from glass with a density of $2485kg/m^3$.

After calibration a set of experiments were conducted each at a different superficial velocity, u_0. After several measurement at different superficial velocities have been made for one powder the tower was emptied and the same procedure was followed with one of the other powders under consideration. Starting with calibration and ending with the actual measurements. All of the measurements made in the present study were taken over a 60s period. According to Makkawi and Wright this is an acceptable experimental span and will produce stable and reliable results [3].

1.3 The reconstruction program

The commercial code *MATLAB* was employed in developing the reconstruction program. For each experiment where 60s of data were recorded a series of 6000 images were produced. These images were organised and sorted and then it was read in, one by one, into the reconstruction program. For each image (which can be viewed as a 'slice' through the reactor) bubbles were recognised, labeled and saved. Information about the bubble diameter, location and shape were also stored into a growing data structure. Then the next image was read in and the same was done except now it was compared to the previous image. By doing this the program could connect these separate images to produce a three dimensional image of

bubbles and other phenomena in a fluidized bed. Quantities like the bubble volume and height could also be determined that would otherwise have been impossible by just using separate images.

The two planes of the ECT system also make it possible to correlate velocities. This could not be done in the present study because of the dramatic changes the fluidized bubbles go through from one measuring plane to the other. Bubble coalesce and split before they reach the second measuring plane. This makes tracing a single bubble no trivial task. If the 6000 recorded images were to be placed one after the other a time stacked image will be produced. This is because it is only time that separates one image being recorded from the next. To convert the time stacked images into a three dimensional image in space only the bubble velocity was needed. Equations predicting the bubble velocity were used to get a semi-empirical estimation of the bubble velocity as described by Kunii and Levenspiel [7]. These equations required the bubble diameter (b_d) as independent variable and the values that were obtained from the reconstruction program was used for this parameter. To estimate the bubble diameter the mean diameter of all the 'slices' of a single bubble was calculated by the program and then the mean of all the bubbles mean diameters were calculated to produce the representative average bubble diameter for a particular experiment.

To determine the bubble velocity three expressions were used that give estimations of the bubble rise velocities in bubbling beds. The bubble velocity for a single bubble is given as

$$u_{br} = 0.711\,(gb_d)^{1/2}, \tag{2}$$

according to the Davidson and Harrison model [8]. For bubbles in a bubbling bed the Davidson and Harrison model states

$$u_b = u_o - u_{mf} + u_{br}, \tag{3}$$

with u_o the superficial velocity and u_{mf} the minimum fluidization velocity. The second equation covers all the particles size distributions, Geldart **A** to **D**, and takes the reactor's diameter into account. This equation was proposed by Werther [7] and is expressed as

$$u_b = \psi\,(u_o - u_{mf}) + \alpha u_{br}, \tag{4}$$

where ψ is the fraction of visible bubbles and α compensates for the differences between a single rising bubble and bubbles rising in a bubbling bed. Empirical estimations for these quantities are described by Kunii and Levenspiel [7]. Kunii and Levenspiel proposed the third correlation and is based on experimental data of Geldart **B** particles in a tower with a diameter less than one meter. This correlation is expressed as

$$u_b = 1.6\left((u_o - u_{mf}) + 1.13b_d^{1/2}\right)d_t^{1.35} + u_{br}, \tag{5}$$

with d_t the tower diameter [7]. According to Kunii and Levenspiel equations (3) to (5) must be calculated and the larger value must be used as the bubble rise velocity, u_b. This procedure was followed in the present study.

2 Results and discussion

To present the result in a clear way a velocity coefficient, v_c, was introduced. This dimensionless quantity made it possible to plot most of the obtained data of a particular parameter in one figure. The coefficient used is defined as

$$v_c = \frac{u_b - (u_o - u_{mf})}{\sqrt{gd_t}}, \tag{6}$$

where u_b is the bubble rise velocity, u_o is the superficial velocity, u_{mf} is the minimum fluidization velocity and d_t is the experimental tower diameter.

In Figure 3(a) the bubble diameter ratio as a function of the velocity coefficient is given and all the data obtained, from both plane one and plane two, followed the same trend. A quadratic fit was also made and presented along with the data. The data and thus the quadratic fit seem to be independent of the height above the distributor. This might seem in contradiction with equation (7) but this apparent independence of z is merely an effect of the velocity coefficient.

Numerous experimental correlations have been developed over the years to estimate the bubble size in a fluidized bed and mainly for small experimental towers with Geldart **B** particles [7]. One such a correlation is given by Werther for Geldart **B** particles that is fluidized through a porous plate distributor and is expressed as [7]

$$b_d = 0.853\left[1 + 0.272\,(u_0 - u_{mf})\right]^{1/3}(1 + 0.0684z)^{1.21}\ \ [cm], \tag{7}$$

where z is the height above the distributor and b_d the bubble diameter. Equation (7) along with data obtained from the 100–200μm powder are given in Figure 3(b).

From Figure 3(b) the correlation between the experimental data and equation (7) is inadequate. One trivial explanation for this inadequate correlation might be because of the definition of the average bubble diameter in the present study (refer to Section 1.3). Usually the bubble diameter, b_d, is defined as the diameter of an equivalent sphere having the same volume as the actual bubble [8]. With the ECT system and the reconstruction program this definition was impractical for the present study. The operating condition of equation (7) is given as follows

$$\begin{aligned} d_t > 20cm, \qquad & 1 \le u_{mf} \le 8cm/s, \\ 100 \le d_p \le 350\mu m, \qquad & 5 \le u_o - u_{mf} \le 30cm/s. \end{aligned}$$

These operating conditions thus does not cover all the parameters of the 100–200μm powder experiments' operating condition and thus discrepancies could be expected.

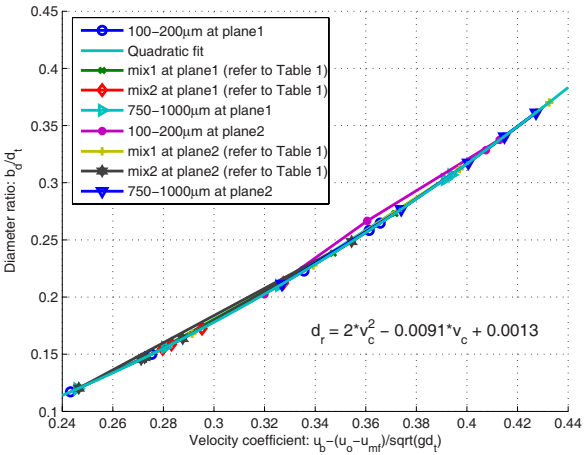

(a)

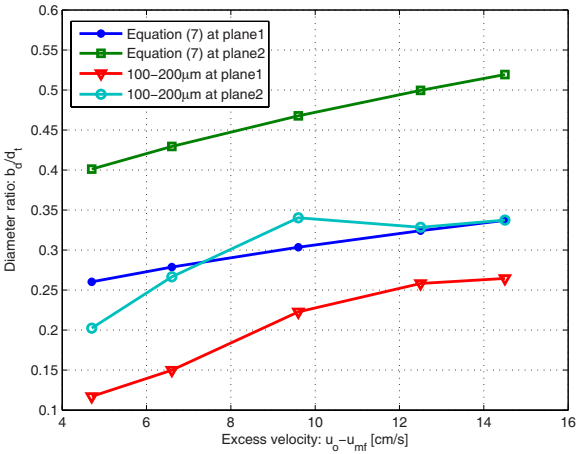

(b)

Figure 3: (a) Dimensionless velocity coefficient against the dimensionless diameter ratio, d_r, for both plane one and plane two. A quadratic fit to the data is also given along with its equation. (b) Theoretical equation (7) against the 100–200μm particles data.

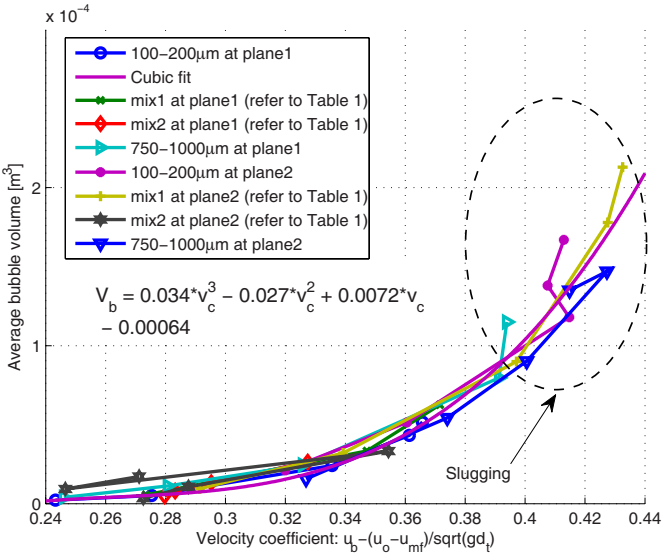

Figure 4: Average bubble volume, V_b, as a function of the velocity coefficient for both plane one and plane two.

From Figure 3 it is not trivial to observe the influence of fines on a powder. Nevertheless the equation produced by the quadratic fit might be a useful tool in determination of the bubble diameter or of the velocity coefficient, depending on which experimental data are available. Overall the fines caused a smaller average bubble diameter which in turn caused a lower bubble rise velocity and thus low velocity coefficient values (refer to Figure 3(a)).

In Figure 4 the average bubble volume is given as a function of the velocity coefficient.

Again very similar behaviour is observed from all the recorded data at plane one and plane two. A cubic fit was found to give a good estimation to all the recorded data points at velocity coefficient values less than 0.38. At velocity coefficient values greater that 0.38 some of the average bubble volume data deviate from the cubic trend. These deviations occurred for all of the data recorded at plane two and for the 750–1000μm powder at plane one as well. These deviation is suspected to be an indication of the onset of the slugging regime. Slugs will cause a lower bubble rise velocity and high average bubble volumes. This is clear in Figure 4 from the higher values of the average bubble volume that was observe for the 100–200μm powder and the *mix 1* powder at plane two and the 750–1000μm powder at plane one. The *mix 2* powder's data at plane two reached a maximum average bubble volume at a velocity coefficient value of about 0.35 and then decreased. This effect is attributed to segregation effects in the bed due to the large particle size distribution that is present. As the superficial velocity is increased

the bed mixes better and thus the bed behaviour can change as is observed with the *mix 2* powder. The average bubble volume for the *mix 2* powder thus stayed low compared to the case where just the 750–1000μm powder was present. It is difficult to observe but the same evidence is present in Figure 3(a). When just the 750–1000μm powder was fluidized; evidence of slugging behaviour occurred even at plane one. The presence of smaller particles or fines in a powder results in an overall smaller average bubble. The last data point of the 750–1000μm powder had a lower velocity coefficient and a lower average bubble volume. This is attributed to a slug that collapsed because of instabilities in the forces that keep the slug's shape. This topic is part of on-going research and is not part of the present study.

3 Conclusion

The influence of fines in powders used in a fluidized bed has been investigated. A range of different powders and powder mixtures have been used and these powders were mainly from the Geldart group **B**. The effect of the fines in powders have been studied by means of the bubble behaviour in the fluidized bed. Using an ECT (Electrical Capacitance Tomography) system data were obtained from a fluidized bed in operation and a reconstruction program developed for the present study was used to calculate characteristics of the bubbles in the bubbling bed. These characteristics were the bubble diameter and volume.

From the result it can be concluded that the insertion of fines into a powder has the effect of smaller average bubble sizes in the fluidized bed. This was observed in both the data obtained for the bubble diameter and volume. It was also evident that fine cause a powder that is prone to slugging to require much larger superficial velocities before signs of slugging set in. This was observed in Figures 3(a) and 4. Fines is thus desirable in Geldart type **D** particles as it suppresses the slugging behaviour that these particles would usually exhibit and instead causes smaller bubbles that would lead to better mixing of the bed content.

Finally, two expressions were correlated using the experimental data. For the diameter ratio the expression is given as

$$d_r = 2v_c^2 - 0.0091v_c + 0.0013, \tag{8}$$

where d_r is the dimensionless diameter ratio (b_d/d_t) and v_c is the velocity coefficient (equation (6)). The expression for the average bubble volume is

$$V_b = 0.034v_c^3 - 0.027v_c^2 + 0.0072v_c - 0.00064, \tag{9}$$

where V_b is the average bubble volume. Deviation from these correlations seem to appear with the on set of the slugging regime. As long as the bed is in the bubbling regime these correlation should given an accurate estimation of the fluidized bed behaviour. Whether these equations are generally adequate is not yet clear and further research is needed to validate these empirical correlations.

References

[1] Qiu, C., Hoyle, B.S. & Podd, F.J.W., Engineering and application of dual-modality process tomography system. *Flow Measurement and Instrumentation*, **18**, pp. 247–254, 2007.
[2] Process tomography Ltd., 86 Water Lane, Wilmslow, Cheshire. SK9 5BB, UK, *PTL300-TP-G ECT system, Operation manual*, 2003.
[3] Makkawi, Y.T. & Wright, P.C., Electrical capacitance tomography for conventional fluidized bed measurements-remarks on the measuring technique. *Powder Technology*, **148**, pp. 142–157, 2004.
[4] Makkawi, Y.T. & Wright, P.C., Fluidization regimes in a conventional fluidized bed characterized by means of electrical capacitance tomography. *Chemical Engineering Science*, **57**, pp. 2411–2437, 2002.
[5] Jayarathna, S.A., *Recommendation of a model for simulating and analysis of the influence of particle size distribution on the simulations of bubbling fluidized beds*. Master's thesis, Telemark University College, 2008.
[6] Rautenbach, C., *Modelling of flow through porous packing elements of a CO_2 absorption tower*. Master's thesis, Stellenbosch University, 2009.
[7] Kunii, D. & Levenspiel, O., *Fluidization Engineering second edition*. Butterworth-Heinemann series in chemical engineering: Oxford, U.K., 1991.
[8] Davidson, J.F. & Harrison, D., *Fluidized particles*. Cambridge University Press: Cambrige, U.K., 1963.